molecular pharmaceutics

pubs.acs.org/molecularpharmaceutics

Article

A Modular Albumin-Oligonucleotide Biomolecular Assembly for Delivery of Antisense Therapeutics

Marwa Elkhashab, Yeter Dilek, Morten Foss, Laura B. Creemers, and Kenneth A. Howard*

Cite This: *Mol. Pharmaceutics* 2024, 21, 491−500

Read Online

ACCESS | Metrics & More | Article Recommendations | Supporting Information

ABSTRACT: Antisense nucleic acid drugs are susceptible to nuclease degradation, rapid renal clearance, and short circulatory half-life. In this work, we introduce a modular-based recombinant human albumin-oligonucleotide (rHA-cODN) biomolecular assembly that allows incorporation of a chemically stabilized therapeutic gapmer antisense oligonucleotide (ASO) and FcRn-driven endothelial cellular recycling. A phosphodiester ODN linker (cODN) was conjugated to recombinant human albumin (rHA) using maleimide chemistry, after which a complementary gapmer ASO, targeting ADAMTS5 involved in osteoarthritis pathogenesis, was annealed. The rHA-cODN/ASO biomolecular assembly production, fluorescence labeling, and purity were confirmed using polyacrylamide gel electrophoresis. ASO release was triggered by DNase-mediated degradation of the linker strand, reaching 40% in serum after 72 h, with complete release observed following 30 min of incubation with DNase. Cellular internalization and trafficking of the biomolecular assembly using confocal microscopy in C28/I2 cells showed higher uptake and endosomal localization by increasing incubation time from 4 to 24 h. FcRn-mediated cellular recycling of the assembly was demonstrated in FcRn-expressing human microvascular endothelial cells. ADAMTS5 in vitro silencing efficiency reached 40%, which was comparable to free gapmer after 72 h incubation with human osteoarthritis patients' chondrocytes. This work introduces a versatile biomolecular modular-based "Plug-and-Play" platform potentially applicable for albumin-mediated half-life extension for a range of different types of ODN therapeutics.

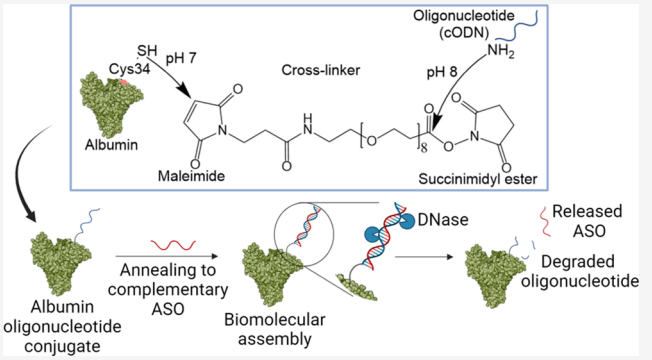

KEYWORDS: *antisense oligonucleotide, albumin, biomolecular assembly, FcRn, ADAMTS5, osteoarthritis*

INTRODUCTION

Antisense oligonucleotide (ASO) drugs interrupt protein expression by engagement with target mRNA[1] using RNase H1-mediated RNA cleavage and RNA blockade.[2,3] ASOs have reached the market for a range of indications that include TEGSEDI for polyneuropathy of hereditary transthyretin-mediated amyloidosis, SPINRAZA for spinal muscular atrophy, and Vyondys 53 for Duchenne muscular dystrophy.[4]

ASOs, however, possess a short plasma circulatory half-life due to nuclease degradation and rapid renal clearance, with biodistribution mostly limited to the liver and kidney. Chemical modifications such as phosphorothioate backbone and ribose sugar modifications including 2′*O*-methyl[5] and 2′*O*-methoxyethyl[6] have been incorporated into the ASO design to increase nuclease resistance and RNA binding affinity. When the design includes modified RNA-based flanking terminal regions such as locked nucleic acids (LNAs) separated by a central DNA sequence, the ASO is referred to as a "gapmer"[2] that exhibits high binding to the target mRNA and unassisted gymnotic cellular delivery.[7,8] ASO modifications have been shown to facilitate a wider tissue distribution of ASOs, exhibiting liver, kidney, pancreas, lymph nodes, spleen, and bone marrow accumulation. Binding of the phosphorothioate backbone to plasma proteins is a proposed mechanism for the broad biodistribution of modified ASOs.[9] However, the kidney remains the predominant accumulation site of these gapmer designs.[9−11]

We have previously shown that acyl-modified phosphorothioated gapmer ASOs with high binding to human serum albumin (HSA) exhibit an extended circulatory half-life and wide tissue distribution, in contrast to albumin nonbinding gapmers.[12] Albumin is the most abundant plasma protein with a broad tissue distribution and a long circulatory half-life of approximately 19 days,[13] predominantly facilitated by engagement with the cellular recycling neonatal Fc receptor (FcRn).[14] These properties have been engineered into albumin-based marketed drugs.[15,16]

Received: June 30, 2023
Revised: November 16, 2023
Accepted: December 4, 2023
Published: January 12, 2024

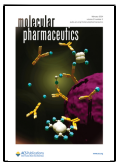

Albumin-based drugs can be categorized into albumin-binding drugs that "hitch-hike" onto the endogenous albumin pool following drug administration, or recombinant human albumin (rHA)-drug fusions or albumin/drug preformulations.[15,16] Endogenous reversible binding albumin drug delivery is an elegant approach for utilizing the inherent properties of albumin, exemplified by the long-lasting effects observed with the marketed insulin and GLP-1 albumin-binding analogues Levemir and Victoza, respectively.

The rHA conjugation and fusion approaches offer designs with more controllable and predictable pharmacokinetics due to nonsusceptibility for displacement by other albumin-binding ligands observed for the noncovalent albumin reversible binding drugs.[15] Furthermore, the identification of rHA sequences engineered with different FcRn affinities offers an unprecedented method to fine-tune the pharmacokinetics, beyond that of harnessing wild-type albumin.[17,18] These variants are based on mutations in specific amino acids of the main FcRn binding interface in domain III of albumin altering FcRn binding to a higher or lower binding affinity to give high binder (HB) and nonbinder (NB) albumin variants, respectively.[19]

The single free thiol displayed on cysteine 34 (Cys34) in albumin domain I presents a site-specific conjugation site distant from the main FcRn binding interface that can be used for albumin functionalization.[20] Our laboratory has developed an albumin-nucleic acid modular biomolecular assembly platform that allows annealing of complementary functionalized oligonucleotide (ODN) modules to the Cys34 site.[21] This assembly has been used by our laboratory to assemble a variety of payloads onto albumin that include fluorophores[21] and cytotoxic drugs[22] attached to the nonfunctional complementary ODN sequence or extending the complementary sequence to include a functional aptamer.

In this work, we extend this approach to directly anneal an ASO as the complementary module sequence that acts as the therapeutic rather than an attachment point, from which a bioactive is subsequently added. The biomolecular assembly was characterized and investigated for serum stability, intracellular trafficking, and ADAMTS5 gene silencing in osteoarthritis (OA) patient chondrocytes to evaluate the therapeutic potential of the design.

EXPERIMENTAL SECTION

Materials. Recombinant human albumin wild-type (WT) and high binder (HB) variants were supplied by Albumedix Ltd. (U.K.).

Oligonucleotides (ODNs) were purchased from Integrated DNA Technologies. Sequences of ADAMTS5-specific ASO (Table 1) and primers (Table 2) were taken from Garcia et al.[23]

Cell Lines and Culture. The C28/I2 human chondrocyte cell line was a kind gift from Prof Goldring at Weill Cornell Medical College (New York). Human articular chondrocytes were isolated from articular cartilage from patients with OA undergoing total knee arthroplasty. The anonymous use of redundant tissue for research purposes is part of the standard treatment agreement with patients in the University Medical Center Utrecht (UMCU) and was carried out under protocol n° 15−092 of the UMCU's Review Board of the BioBank. C28/I2 cells were cultured in Dulbecco's Modified Eagle Medium/Nutrient Mixture F-12 (DMEM/F-12, Gibco, cat# 11320033) with 10% fetal bovine serum (FBS, Gibco, cat# 10500−064), 1% penicillin/streptomycin (P/S, Gibco, cat# 15140−122), and 200 μM L-ascorbic acid 2-phosphate sesquimagnesium salt hydrate (TCI, cat# A2521). Primary chondrocytes were cultured in DMEM (with 4.5 g/L D-Glucose + Pyruvate) (Thermo Fischer Scientific, cat# 31966−021) with 10% FBS (Biowest, cat# S181H), 100 U/mL P/S, 0.2 nM L-ascorbic −2-phosphate sesquimagnesium salt hydrate (Sigma-Aldrich, cat# A8960), and 1 ng/mL basic fibroblast growth factor (bFGF, R&D Systems, cat# 233-FB/CF). Seeding of primary cells was performed in DMEM (with 4.5 g/L D-Glucose + Pyruvate) supplied with 4 g/L human serum albumin (HSA), 1× Insulin-Transferrin-Selenium-Ethanolamine (ITS-X, Thermo Fischer Scientific, cat# 51500056) and 100 U/mL P/S.

Human microvascular endothelial cells (HMEC-1-FcRn) overexpressing human FcRn[14] were used. The cells were cultured in MCDB131 medium (without L-glutamine) (Life Technologies, cat# 10372−019), containing 10% FBS, 2 mM L-glutamine (Lonza, cat# BEBP17−605E), 10 ng/mL human epidermal growth factor (hEGF) (Peprotech, cat# AF-100−15), 1 μg/mL hydrocortisone (Sigma-Aldrich, cat# H0888), 50 μg/mL Geneticin (Gibco, cat# 10131−035), and 0.25 μg/mL puromycin (Life Technologies, cat# A11138−03).

Oligonucleotide Conjugation to rHA. Amino-modified ODNs were mixed with dimethyl sulfoxide (DMSO, Sigma-Aldrich, cat# 34869), 0.1 M 4-(2-hydroxyethyl)-1-piperazineethanesulfonic acid (HEPES, Sigma-Aldrich, cat# H4034) pH 8, and 50× molar equiv of cross-linker succinimidyl-[(N-maleimidopropionamido)-octaethyleneglycol] ester (SM-(PEG)$_8$, Sigma-Aldrich, cat# 746207) overnight at 650 rpm, room temperature (RT). The ODN-linker conjugate was then purified from an unreacted linker using ethanol precipitation and mixed with 2× molar equiv rHA in HEPES buffer (pH 7) overnight. The maleimide linkage was hydrolyzed afterward to prevent a reversible retro-Michael reaction, by addition of Trizma base (tris base, Sigma-Aldrich, cat# T1503−500G) buffer (pH 9) and incubating overnight at 37 °C. The formed conjugate was then purified with HPLC.

Annealing of an Antisense Oligonucleotide Module. The ASO ODN was annealed to its complementary rHA-conjugated oligonucleotide (cODN), by direct mixing of rHA conjugate and ASO in annealing buffer (200 mM potassium acetate) at a 1:1 molar ratio and incubating for 10 min, 1, 2, 3, and 4 h, and overnight. In a separate experiment, non-cODN conjugated rHA and ASO were incubated together in

Table 1. Oligonucleotides Sequences Used (* = Phosphorothioate, + = Locked Nucleic Acid (LNA))

ADAMTS5-specific ASO	5′-NH_2 + C* + T* + T*T*T* A*T*G* T*G*G* G*+T*+T* + G
cODN	5′- NH_2-CA ACC CAC ATA AAA G
mismatch ASO	+G* + G* + A*A*A*C*A*T*C*G*A*C*+A* + G* + T

Table 2. Sequences of Primers Used for RT-qPCR

ADAMTS5	forward	5′ GCCAGCGGATGTGTGCAAGC 3′
	reverse	5′ ACACTTCCCCCGGACGCAGA 3′
GAPDH	forward	5′ TGCACCACCAACTGCTTAGC 3′
	reverse	5′ GGCATGGACTGTGGTCATGAG 3′
18S	forward	5′ GTAACCCGTTGAACCCCATT 3′
	reverse	5′ CCATCCAATCGGTAGTAGCG 3′

https://doi.org/10.1021/acs.molpharmaceut.3c00561
Mol. Pharmaceutics 2024, 21, 491−500

annealing buffer at a 1:1 molar ratio for 10 min, 1, 2, 3, and 4 h, and overnight for assessment of nonspecific binding. The rHA-cODN conjugate and biomolecular assembly protein concentrations were determined by a bicinchoninic acid (BCA, Thermo Scientific, cat# 23225) assay according to the manufacturer's protocol.

Fluorophore Labeling of Oligonucleotides and rHA. Oligonucleotides (ASO and cODN) modified at the 3′ end with an amino group were labeled with an N-hydroxy succinimide-modified fluorophore (fluorophore-NHS). The fluorophore-NHS (either Cy3-NHS or Cy5.5-NHS) (Lumiprobe, cat# 21020 and 47020, respectively) was mixed with the ODN in the presence of DMSO and 0.1 M HEPES (pH 8) and then incubated overnight at 650 rpm at RT. Excess fluorophore and unconjugated ODN were removed using ethanol precipitation[22] and reversed-phase high-performance liquid chromatography (RP-HPLC), respectively. The fluorophore-labeled ODN concentration was determined by measuring the absorbance at 260 nm with a correction factor (CF_{260}) of 0.04 for Cy3-NHS and 0.07 for Cy5.5-NHS.

rHA was labeled nonspecifically on the amino groups of lysine residues. rHA-cODN conjugate or the rHA-cODN/ASO biomolecular assembly was mixed with the fluorophore-NHS in HEPES buffer (pH 8) and incubated overnight at 650 rpm at RT. Excess fluorophore was then removed by spin filtration through a 10 kDa cutoff membrane filter (Amicon Ultra, Merck Millipore Ltd., cat# UFC501096).

HPLC Purification of Labeled Oligonucleotides, rHA Conjugates, and Assemblies. *Ion Exchange Chromatography (IEX).* A Mono Q 5/50 GL column (Sigma-Aldrich) was used for the purification of the rHA conjugates and assemblies. The mobile phase was composed of two buffers (pH 7.6) [Buffer A, 10 mM NaCl (Acros organics, cat# 207790010) and 20 mM Trizma hydrochloride (Tris HCl, Sigma-Aldrich, cat# T5941−500G), Buffer B, 800 mM NaCl and 20 mM Tris HCl]. The elution of rHA-cODN conjugates was performed through a 25 min gradient increase in Buffer B. For purifying rHA-cODN/ASO assemblies, high salt buffer B (3 M NaCl and 20 mM Tris HCl) was used.

The obtained fractions were then desalted using spin filtration, where the samples were washed with PBS through 10 or 30 kDa cutoff membrane filters (Amicon Ultra, Merck Millipore Ltd., cat# UFC501096 & UFC503096).

Reversed-Phase Chromatography (RP-HPLC). A reversed-phase C-18 column (Xterra MS C_{18} 5 μm) was used for purifying fluorophore-labeled ODNs. The mobile phase was composed of 2 buffers [Buffer A: 5% TEAA (triethylammonium acetate, Sigma-Aldrich, cat# 69372) and 5% acetonitirile (VWR, cat# 83639.320), Buffer B: 100% acetonitrile].

The obtained fractions were then speed vacuumed and resuspended in nuclease-free water (NFW, Invitrogen, cat# AM9937).

Polyacrylamide Gel Electrophoresis (PAGE). Native polyacrylamide gels were prepared by mixing ProtoGel (National Diagnostics, cat# EC-890), Milli-Q water, 10× tris, borate, ethylenediamine tetraacetic acid (EDTA) (TBE, Thermo Fisher Scientific, cat# 15581−044), 10% ammonium persulfate (APS) (Sigma-Aldrich, cat# A3678), and *N*,*N*,*N*′,*N*′-tetramethylethylenediamine (TEMED, Sigma-Aldrich, cat# T9281). The mixture was cast on 1 mm gel cassettes (Invitrogen, cat# NC2010) and then incubated at RT for 45 min to allow polymerization.

The samples were mixed with loading buffer to reach a concentration of 10% glycerol (VWR, cat# 24388.295) and 1 g/L Orange G (Sigma-Aldrich, cat# O3756). The gel was run in a TBE buffer at 150 V for 30−90 min using an EPS 601 electrophoresis power supply (Amersham Biosciences). The gel was stained with 1× SYBR Gold (Invitrogen, cat# S11494) for 15 min. A Gel Doc EZ Imager (Bio-Rad) was used for visualizing SYBR Gold staining, and Amersham typhoon 5 (Cytiva), for SYBR Gold and fluorescence imaging.

Antisense Oligonucleotide DNase-Triggered Release. DNase I (DNA-free Kit TURBO, Thermo Fischer, cat# AM1907) was incubated at 1 U/sample with 200 pmols of rHA-cODN/ASO biomolecular assembly in 0.1 volume 10× TURBO DNase buffer at 37 °C for 30 min. 20 pmols of the product were then run on an 8% native polyacrylamide gel at 150 V for 30 min. The ODNs were visualized with SYBR Gold staining.

Serum Stability of the Biomolecular Assembly. rHA-cODN/ASO (Cy5.5) biomolecular assembly stability in 50% human serum was examined at different time points. The assembly was incubated with serum at 37 °C for 0, 12, 24, 48, and 72 h. After each time point, the assembly was frozen at −20 °C until the last time point. Each sample was diluted five times with NFW and run onto 8% native gel and imaged for Cy5.5 fluorescence.

Cellular Localization of the Biomolecular Assembly. For subcellular localization experiments, a dually labeled assembly was used with ASO labeled with Cy5.5 at the 5′ end and rHA labeled with Cy3. C28/I2 cells were seeded overnight at 10,000 cells/well in an 8-well chamber slide (Sarstedt, cat# 94.6140.802) at 37 °C, 5% CO_2. The cells were then treated with the dually labeled assembly at 100 nM and incubated for further 4, 6, and 24 h at 37 °C, 5% CO_2. Cells were washed with DPBS and then fixed with formalin 10% (Sigma-Aldrich, cat# HT5014) for 20 min. After further washing, cells were permeabilized with 0.1% Triton X-100 (Cell Biolabs, INC., cat# 124102) for 20 min, followed by blocking with 5% bovine serum albumin (BSA, Sigma-Aldrich, cat# A9647) in DPBS for 1 h. Cells were washed and incubated with primary rabbit polyclonal antibodies (Abcam), (anti-EEA1, cat# ab2900, for early endosomes, and anti-Lamp1, cat# ab24170, for lysosomes) in 5% BSA at 4 °C overnight. The cells were then washed and incubated with goat antirabbit secondary antibody, Alexa Fluor 488 (Invitrogen, cat# A11034) for 90 min, followed by washing and mounting the slide with UltraCruz Aqueous Mounting Medium with DAPI (Santa Cruz Biotechnology, Inc., cat# sc-24941). The slides were kept at 4 °C in the dark until visualization on a Zeiss Confocal microscope LSM 700 (Carl Zeiss Micro-Imaging). Images were processed with Zeiss Zen Black 2012 edition.

Cell Viability. C28/I2 cells were seeded overnight at 5000 cells/well in a 96-well plate at 37 °C and 5% CO_2. The following day, cells were treated and incubated for a further 72 h at 37 °C, 5% CO_2.

A 3-(4,5-dimethylthiazol-2-yl)-2,5-diphenyltetrazolium bromide (MTT) assay was performed. The medium was removed, and cells were incubated with 100 μL of 0.5 mg/mL MTT reagent (Invitrogen, cat# M6494) in Roswell Park Memorial Institute medium (RPMI, Gibco, cat# 61870−010) for 1 h. The MTT reagent was then removed, and the formazan crystals were dissolved with 100 μL of DMSO. The absorbance was measured at 570 nm for formazan and 650 nm for

https://doi.org/10.1021/acs.molpharmaceut.3c00561
Mol. Pharmaceutics 2024, 21, 491−500

background and compared to untreated cells using a Clariostar plate reader.

FcRn-Driven Cellular Recycling of the Assembly. A 48-well plate (Sarstedt, cat# 83.3923) was coated with Geltrex (Thermo Fisher Scientific, cat# A1413202) for 1 h at 37 °C, 5% CO_2, and then, HMEC-1-FcRn cells were seeded at 100,000 cells/well and incubated overnight at 37 °C, 5% CO_2. rHA conjugates and assemblies were diluted in HBSS adjusted with 1 M 2-(*N*-morpholino) ethanesulfonic buffer (MES, Sigma-Aldrich, cat# M1317) to pH 6. The cells were washed with prewarmed PBS and treated with 150 nM concentration of different rHA variant designs and incubated for 1 h at 37 °C (pH 6), 5% CO_2. Afterward, cells were washed five times with ice-cold PBS and then incubated with serum lacking medium for 1 h at 37 °C, 5% CO_2. The supernatant was collected and the level of recycled rHA was measured using a sandwich enzyme-linked immunosorbent assay (ELISA).

For the ELISA analysis, a 96-well maxisorp plate (Thermo Scientific, cat# 442404) was coated for 2 h at RT with polyclonal goat antihuman albumin antibody (Sigma-Aldrich, cat# A7544) (1:1000) diluted in PBS. The plate was then washed with PBS-0.05% Tween-20 (PBST, Medicago AB, cat# 09−9410−100) and blocked with 2% skimmed milk (Sigma-Aldrich, cat# 70166) in PBS for 2 h. rHA standard solutions and recycled rHA were allowed to bind to the antibody overnight at 4 °C followed by washing with PBST. An HRP-conjugated secondary polyclonal sheep antihuman albumin antibody (Abcam, cat# ab8941) in 2% skimmed milk was added to the plate and incubated for 1 h at RT. After washing, 3,3′,5,5′-tetramethylbenzidine (TMB) (Sigma-Aldrich, cat# T0565) was added to allow the enzymatic reaction to occur. The reaction was stopped with 0.2 M sulfuric acid (H_2SO_4), and the absorbance was measured at 450 nm using a Clariostar plate reader.

ADAMTS5 Gene Silencing in Primary Chondrocytes. Primary chondrocytes were seeded at 100,000 cells/well, passage number 2−3 and attached overnight at 37 °C, 5% CO_2. Cells were treated with 500 nM ADAMTS5-specific ASO, rHA-cODN/ASO biomolecular assembly, rHA-cODN conjugate, and naked mismatch for 72 h. After 10 h of treatment, cells were stimulated with 10 ng/mL TNF-α and 1 ng/mL oncostatin M (OSM).[23] After 72 h, mRNA expression was determined by RT-qPCR. Briefly, total RNA was isolated with TRIzol (Invitrogen, cat# 15596026) and reverse transcribed to cDNA by a High-Capacity cDNA Reverse Transcription Kit (Applied Biosystems, cat# 4368813) using an iCycler Thermal Cycler (Bio-Rad) according to the manufacturer's protocol. The cDNA was amplified with iTaq Universal SYBR Green Supermix (Bio-Rad, cat# 1725124) in an iCycler CFX384 Touch thermal cycler (Bio-Rad). 2 μL of five times diluted cDNA was added to 18 μL of reaction mixture containing 0.4 μM forward and reverse primers and 10 μL of iTAQ Universal SYBR Green Supermix (2×). A three-step amplification qPCR was used for the analysis of gene expression including the ADAMTS5 gene and housekeeping genes (GAPDH and 18S). Ct values were obtained by a Bio-Rad CFX Manager 3.1, and relative gene expression was calculated with a PfaffI method to account for primers' efficiencies. Statistical analysis of the results was performed by a one-way ANOVA test using GraphPad prism 9.5.0 software.

RESULTS

A DNA ODN (linker strand) was conjugated to rHA (rHA-cODN) after which it was annealed to a complementary ASO to form the rHA-cODN/ASO biomolecular assembly. Both the rHA-cODN conjugate and the rHA-cODN/ASO were purified by IEX HPLC (Figures S1 and S2). DNA ODN conjugation and ASO annealing were determined by the band migration shift on a native PAGE (Figure 1). The free ODNs migrated

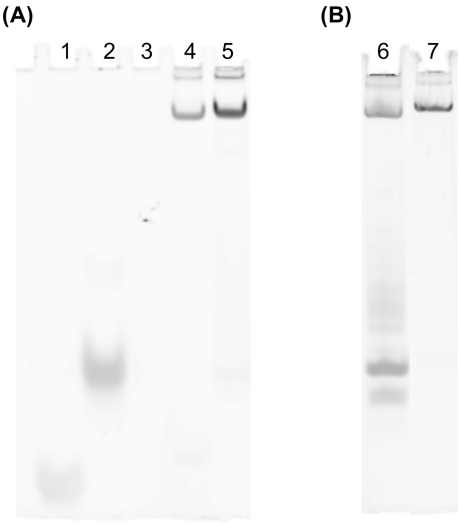

Figure 1. SYBR Gold imaging of 15% native gel, showing the different assembly steps of the design. Gel (A) shows the purified products. Lane 1: cODN, lane 2: ASO, lane 3: rHA, lane 4: rHA-cODN conjugate, and lane 5: rHA-cODN/ASO biomolecular assembly. Gel (B) shows the difference between the rHA-cODN conjugate before and after HPLC purification. Lane 6: nonpurified assembly. Lane 7: purified assembly. Bands in the upper half of the gel represent rHA, rHA-cODN conjugate, and rHA-cODN/ASO assembly, while bands in the lower half of the gel represent naked oligonucleotides.

further in the gel compared to that of the albumin-associated ODN (Figure 1A). The biomolecular rHA-cODN/ASO assembly band (lane 5) showed a slight retardation compared to the rHA-cODN conjugate band (lane 4). In Figure 1B, no ODN bands were observed at the bottom of the gel in the HPLC-purified rHA-cODN conjugate (lane 7) compared to the nonpurified control (lane 6).

Thiol-specific conjugation was confirmed by analysis of native PAGE shown in (Figure S3). No conjugation was observed (Figure S3, lane 2) when the maleimide cross-linker was prehydrolyzed before addition of rHA, confirmed by the absence of a visible rHA-cODN band in the upper half of the gel.

A Cy5.5-labeled ASO was annealed to the conjugate at different time points to determine the kinetics and efficiency of annealing. In addition, nonconjugated rHA was incubated with the labeled ASO to evaluate any nonspecific, noncovalent association. Both the labeled ASO and assembly were detected by fluorescence imaging on native PAGE (Figure 2A,B). In Figure 2A, the lower bands of the gel represent the nonannealed ASO, while the upper bands show the annealed ASO or any nonspecifically bound ASO. The band intensity of the nonannealed ASO decreased with an increase in incubation time, with the lowest intensity observed after overnight annealing. The percentage of annealing or any nonspecific binding was calculated (Figure 2C) by comparing the intensity

https://doi.org/10.1021/acs.molpharmaceut.3c00561
Mol. Pharmaceutics 2024, 21, 491−500

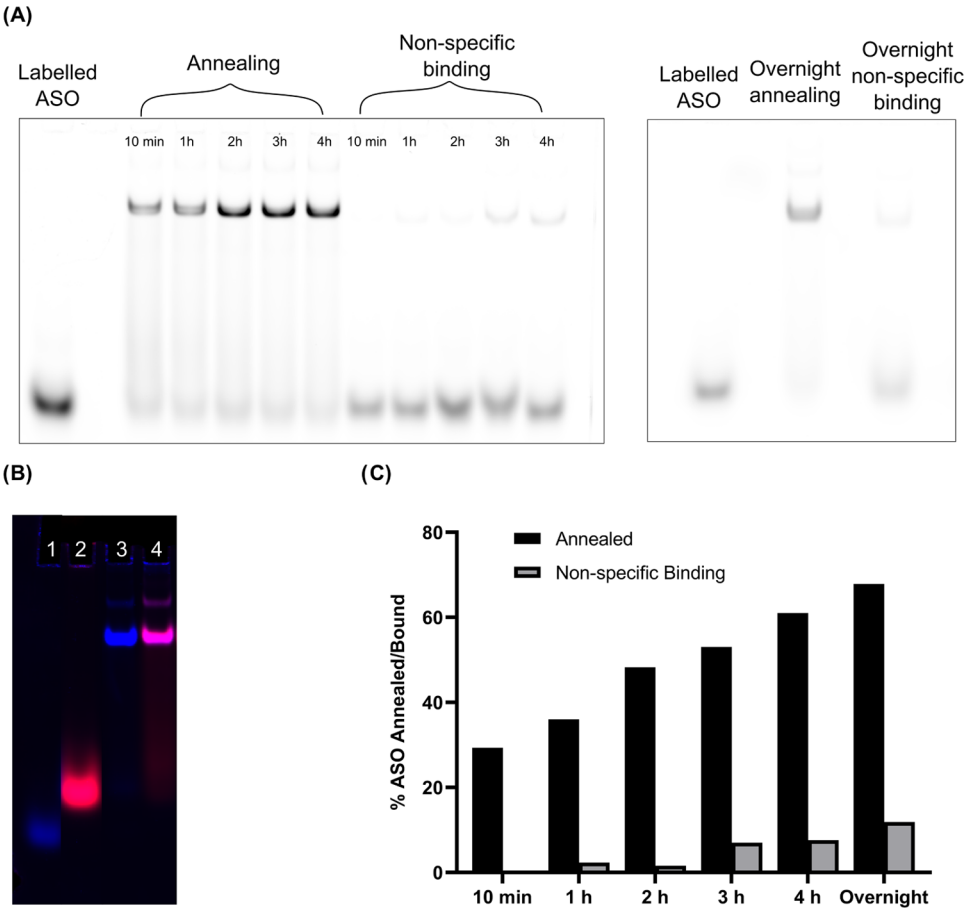

Figure 2. (A) Cy5.5 fluorescence imaging of 8% native gel showing different time points for annealing and nonspecific binding of the rHA-cODN conjugate and rHA respectively with Cy5.5-labeled ASO at a 1:1 molar ratio. (B) A combined image of Cy5.5 fluorescence and SYBR Gold imaging of Cy5.5-labeled assembly produced after overnight annealing. Lane 1: cODN (SYBR Gold, blue), Lane 2: Cy5.5-labeled ASO (red), Lane 3: rHA-cODN conjugate (SYBR Gold, blue), Lane 4: labeled biomolecular assembly colocalization of SYBR Gold and Cy5.5 signals (purple). (C) The percentage (%) of annealing and nonspecific binding between the rHA-cODN conjugate and rHA respectively with Cy5.5-labeled ASO. A bar chart was generated utilizing data obtained from a single experiment (N = 1) and was created using GraphPad prism software 9.5.0.

of the upper band (annealed or nonspecific bound ASO) to the total intensity of both the lower (free ASO) and upper bands. The calculated percentage of annealing increased by prolonged incubation, reaching 61% after 4 h and 67.9% when incubated overnight. In contrast, nonspecific binding only reached ∼ 11% after overnight incubation.

The Cy5.5-labeled biomolecular assembly was additionally labeled with Cy3 on the surface lysines of rHA for subsequent dual imaging experiments. A native PAGE showed colocalization of both Cy5.5 and Cy3 components (Figure 3A).

The rHA-cODN/ASO biomolecular assembly disassembly and consequent ASO triggered release following incubation with DNase I were investigated in a native PAGE gel. Following 30 min of incubation with DNase I, the ASO was almost completely released from the assembly, showing a lower ASO band compared with the assembly before DNase I incubation (Figure 3B).

The release of a Cy5.5-labeled ASO from the assembly in the presence of 50% human serum was determined at different time points in an 8% native gel (Figure 4A). In the presence of serum, the migration of the rHA-cODN/ASO biomolecular assembly in the gel was slightly slower compared to the control assembly without serum. The percentage of assembly remaining intact in serum was calculated by band fluorescence intensity analysis of the assembly at different time points

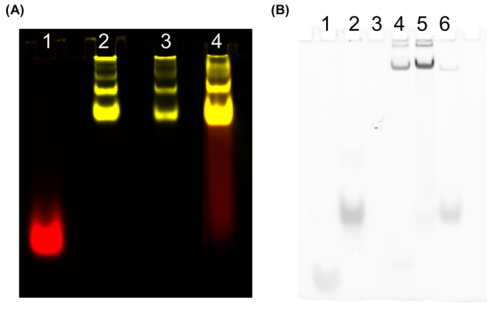

Figure 3. (A) Cy5.5/Cy3 fluorescence imaging of 8% native gel showing different fluorescent constructs. Lane 1: Cy5.5-labeled ASO (red), Lane 2: Cy3-labeled rHA (yellow), Lane 3: Cy3-labeled rHA-cODN conjugate (yellow), Lane 4: labeled assembly (Cy3-labeled rHA and Cy5.5-labeled ASO) (deeper yellow/orange). (B) SYBR Gold imaging of 15% native gel showing ASO release from the assembly following DNase I incubation. Lane 1: cODN, Lane 2: ASO, Lane 3: rHA, Lane 4: rHA-cODN conjugate, Lane 5: rHA-cODN/ASO biomolecular assembly, Lane 6: rHA-cODN/ASO biomolecular assembly after DNase I treatment.

compared to the zero time point. Approximately 60% of the assembly remained intact after 72 h of incubation in serum (Figure 4B).

https://doi.org/10.1021/acs.molpharmaceut.3c00561
Mol. Pharmaceutics 2024, 21, 491−500

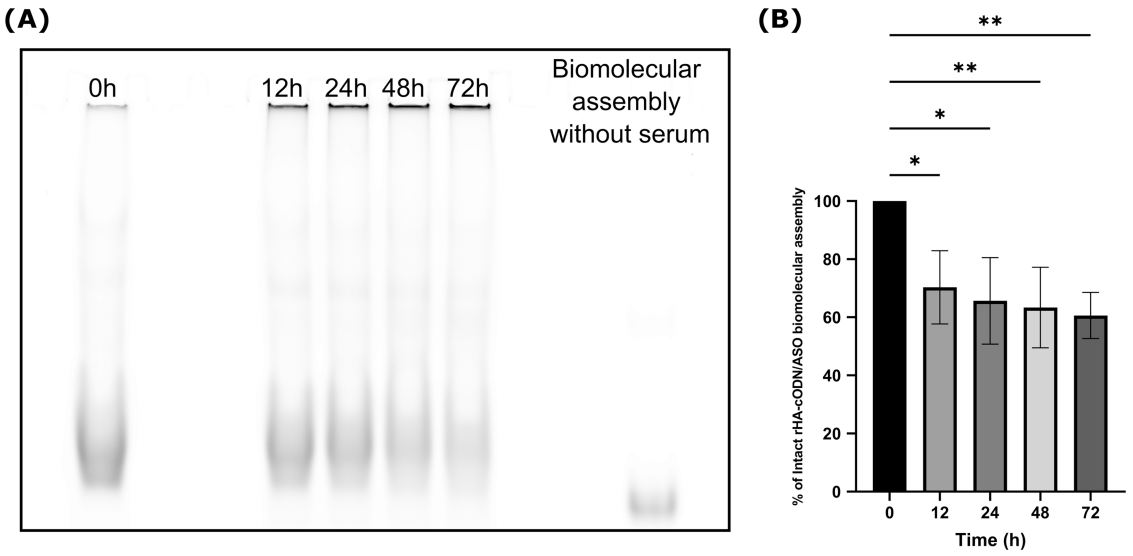

Figure 4. ASO release from the rHA-cODN/ASO biomolecular assembly in 50% human serum. (A) Cy5.5 fluorescence imaging of 8% native gel showing the serum stability of the biomolecular assembly at different time points. (B) Percentage of biomolecular assembly remaining intact after incubation with serum. The % is calculated by ImageJ, and the error bars represent the standard deviation of three independent experiments (N = 3). A bar chart was created using GraphPad prism software 9.5.0, and statistical analysis was performed using the one-way Anova test, ** = p < 0.01, * = p < 0.05.

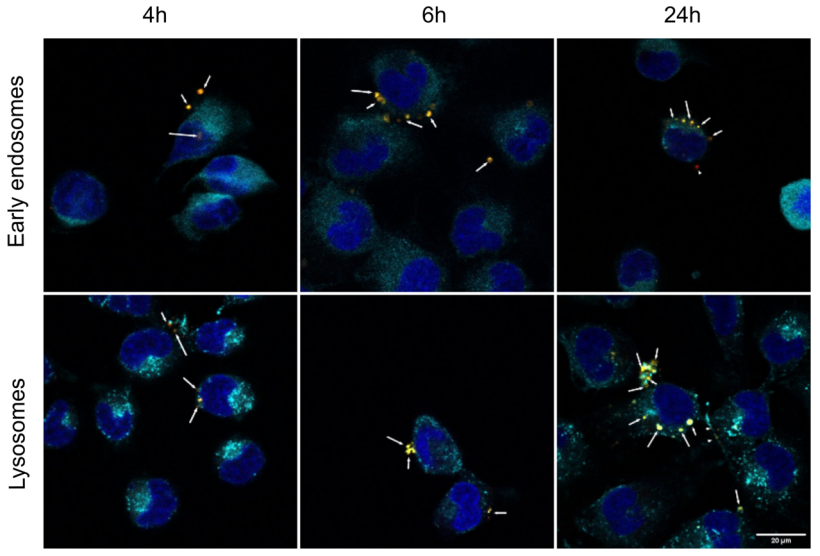

Figure 5. Confocal images of dually labeled rHA-cODN/ASO biomolecular assembly subcellular localization in C28/I2 cells after 4, 6, and 24 h. Nuclei stained with DAPI (blue) and endosomal staining (cyan) performed by rabbit polyclonal antibody (anti-EEA1 for early endosomes and anti-Lamp1 for lysosomes) followed by AF488 goat antirabbit polyclonal antibody. Cy5.5-labeled ASO is depicted in red, Cy3-labeled rHA in yellow, the assembly in orange or deep yellow, and the assembly colocalizing with endosomes in the green to white color range. Arrows indicate assembly, and arrowheads indicate single ASO (Cy5.5) or rHA (Cy3) molecules. Scale bar: 20 μm. Images were processed with ImageJ 1.53q.

The biomolecular assembly cellular internalization, trafficking, and disassembly over time were determined by confocal microscopy in C28/I2 cells (Figure 5). After 4 h, an intact assembly (demonstrated by the colocalization of the rHA (Cy3) and ASO (Cy5.5) fluorescent labels) exhibited internalization and localization within early endosome and lysosome that increased at 6 h. Intact assembly in addition to a few single ASO and rHA molecules was apparent at 24 h. Detailed confocal images are shown in Figures S6–S8.

An MTT cytotoxicity assay was performed on the C28/I2 human chondrocyte cell line to determine the cellular compatibility of the assembly at concentrations used in cellular gene silencing work. Over a 72 h incubation period, there was no apparent toxicity observed up to a 500 nM concentration. In addition, the ASO alone and a mismatch did not exhibit any cytotoxicity over the 72 h incubation period at concentrations reaching 1 μM (Figure S5).

FcRn-mediated endosomal cellular recycling was investigated for the rHA-cODN conjugate, biomolecular assembly, and rHA in HMEC-1-FcRn cells overexpressing human FcRn. High FcRn-binder (HB) rHA showed statistically significant more recycling than its wild-type (WT) rHA counterpart. The attachment of ODNs to rHA slightly reduced recycling compared to the nonconjugated rHA variant (Figure 6).

A cellular gene silencing experiment was performed to determine whether the ASO gene silencing functionality was

https://doi.org/10.1021/acs.molpharmaceut.3c00561
Mol. Pharmaceutics 2024, 21, 491−500

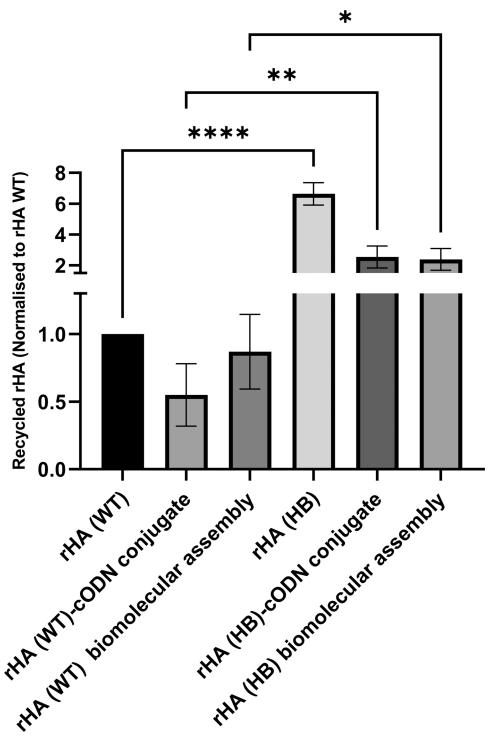

Figure 6. Cellular recycling assay of rHA-oligonucleotide designs in HMEC-1-FcRn cells. Results are normalized to rHA WT. Error bars represent the standard deviation of three independent experiments (N = 3) (each was performed in triplicate). A bar chart was created using GraphPad prism software 9.5.0, and statistical analysis was performed using the one-way Anova test, *** = $p < 0.001$, ** = $p < 0.01$, * = $p < 0.05$.

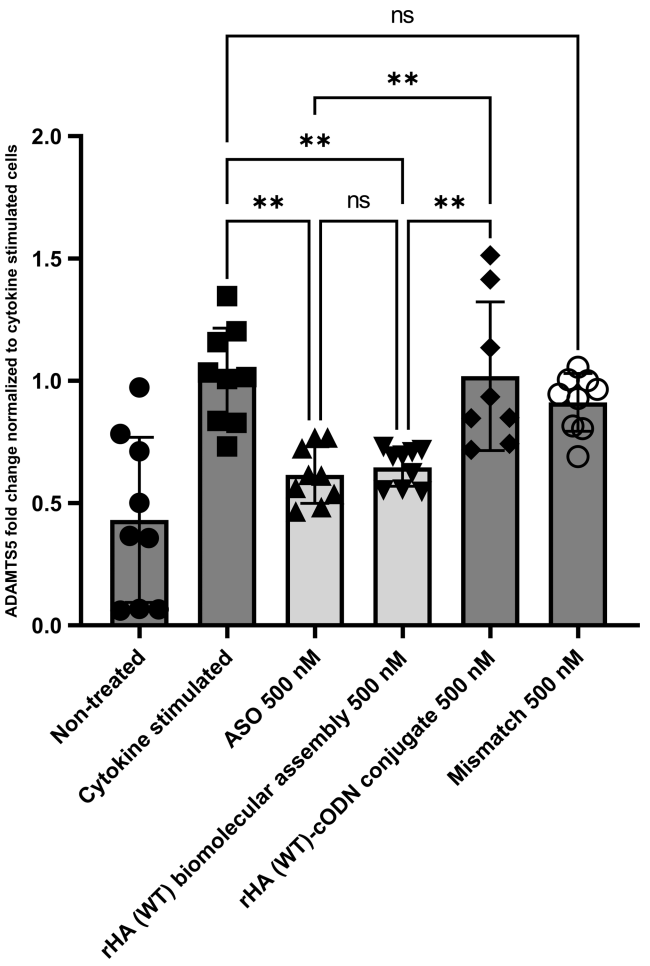

Figure 7. ADAMTS5 gene silencing efficiency in human primary chondrocytes. An rHA-cODN conjugate and ASO mismatch were used as negative controls. ADAMTS5-specific ASO was used as a positive control. Results are normalized to cytokine-stimulated cells. Error bars represent the standard deviation of three independent experiments (N = 3) (each experiment was performed in triplicate). Each independent experiment was performed on primary human chondrocytes obtained from a different donor. A bar chart was created using GarphPad prism software 9.5.0, and statistical analysis was performed using the one-way Anova test, ** = $P < 0.01$, ns = nonsignificant.

retained following incorporation into the biomolecular assembly design. Gene silencing was performed on primary human chondrocytes stimulated with TNF-α and oncostatin M to simulate the inflammatory osteoarthritic environment that leads to overexpression of ADAMTS5.

ADAMTS5 silencing of the rHA-cODN/ASO biomolecular assembly was comparable (nonsignificant difference) to the silencing efficiency of the naked ASO (Figure 7). Both the ASO and the assembly showed ~40% ADAMTS5 gene silencing, which was significant ($P < 0.01$) in comparison to the cytokine-stimulated control cells.

DISCUSSION

Antisense oligonucleotides are synthetic therapeutic DNA molecules that have reached the clinic.[4,24] Backbone modifications have been introduced into ASOs to meet the challenges of inadequate stability and short circulatory half-life. Phosphorothioate modifications have been suggested to mediate binding to serum proteins that improve the half-life extension and biodistribution of ASOs. However, phosphorothioated ASOs still mainly accumulate in the kidney.[11] In addition, ASO sequence-dependent variations in protein binding affinities can lead to variable biodistribution.[10] This work aimed to develop an albumin delivery system for ASOs based on conjugating ASOs to recombinant albumin variants to enable controlled and programmable FcRn-driven increased circulation of ASOs regardless of the differences in ASO protein binding affinities.

Previous work by our lab introduced the use of ODNs as linkers onto which different payloads can be added to rHA.[21] The system is based on a short DNA ODN linker strand conjugated to rHA, onto which a complementary DNA ODN conjugated to a functional moiety is annealed. This was exemplified to incorporate an anticoagulant nucleic acid RNA aptamer sequence that was extended from the nonfunctional complementary sequence of the assembly. In this work, we replaced the complementary ODN linker directly with a therapeutic ASO.

An ODN was conjugated using standard maleimide chemistry to the single free thiol positioned in domain I, lying distant from the main FcRn binding interface in albumin domain III.[15] A hydrolysis step was performed to avoid a maleimide retro-Michael reaction and consequent instability.[25] The hydrolysis of the maleimide cross-linker before addition of rHA did not result in any observed conjugation, which suggests that the rHA-cODN conjugate is likely a product of the interaction between the maleimide group and the single available free thiol at Cys34, lying in domain I of rHA. Future work could employ an alternative monobromo maleimide

https://doi.org/10.1021/acs.molpharmaceut.3c00561
Mol. Pharmaceutics 2024, 21, 491−500

(MBM) linker used in our previous work[22] where a thiomaleimide is formed after conjugation, resulting in a stable nonreversible conjugate with a higher maleimide hydrolysis rate.

Formation of the DNA duplex can be achieved either by thermal annealing or time based annealing at room temperature (RT); however, in the presence of albumin, RT annealing was preferred to avoid possible albumin denaturation.[26] Previous work has showed the ability of phosphorothioated ODNs to bind to proteins,[12] confirmed in this work with ∼ 11% of the gapmer ASO exhibiting noncovalent association with rHA. However, this percentage was low compared to gapmer ASO attachment that reached 68% through complementary base pair annealing. The incorporation of the phosphorothioate backbone required a strong eluting buffer for IEX purification; therefore, a 3 M salt buffer was used to elute the assembly.[27] The ability to attach fluorophores to both ODN strands in the assembly offers the possibility to further functionalize the design with, for example, targeting ligands.

Conjugation of ASOs to ligands such as tocopherol[28] or a lipophilic tail[29] has been shown previously to reduce gene silencing, possibly due to steric hindrance of mRNA engagement. In our work, the ASO is noncovalently annealed to an rHA-conjugated complementary DNA linker strand susceptible to DNase degradation that can be exploited for DNase-triggered ASO release from the assembly. This may have implications such as premature in vivo release; however, up to 60% of the assembly remained intact after 72 h of incubation in 50% human serum. Moreover, it would be expected that greater degradation would occur intracellularly due to the combined presence of both DNase I and II nucleases.[30,31] Some high molecular weight (Mw) bands nonmigrating in the native PAGE were observed after incubating the assembly in serum. These bands could indicate a degree of aggregation possibly due to interaction of serum proteins with the assembly; however, these represent only around 30% of the assembly. The substantial release of ASO observed after 30 min of DNase treatment was likely a result of the use of a recombinant DNase I (TURBO DNase), which is significantly more efficient than the wild-type DNase I in digesting DNA. The incorporation of LNA and PS modifications, as expected, conferred stability to the released ASO in the presence of TURBO DNase.

Gapmer ASOs exhibit cellular internalization without the requirement for transfection agents, by a process of gymnosis.[7,8] The cellular trafficking of ASO after incorporation into an rHA biomolecular design was investigated in our work by confocal microscopy. The images suggest endosomal uptake of the assembly that likely reflects the reported FcRn-driven endosomal recycling pathway of albumin.[14] This was supported by a cellular recycling assay. Despite conjugation at Cys34 in albumin domain I, distant from the main FcRn binding interface in domain III, the recycling assay showed less recycling of rHA in the conjugated form than that of its free rHA counterpart. The recycling, however, was higher for an FcRn-high binding (HB) rHA assembly, than its WT counterparts, due to the presence of mutations at HB rHA domain III, known to confer higher binding affinity for FcRn.[14] These results suggest that the inclusion of HB rHA into the biomolecular design may offer more effective FcRn-driven cellular recycling half-life extension. These results are consistent with our previous work, where payloads on Cys34 of albumin were shown to reduce FcRn binding affinity compared to free albumin, but restored using FcRn-high binding human recombinant albumin variant.[32,33] Interestingly, in our previous work with albumin conjugated to a different ODN sequence,[22] albumin recycling showed an increase that could reflect ODN binding to cellular receptors influenced by ODN length and specific ODN sequences.

The therapeutic potential of this ODN delivery platform was exemplified in this work using an ASO gapmer against the ADAMTS5 enzyme involved in osteoarthritis. The biomolecular assembly exhibited ∼40% knockdown of ADAMTS5 in osteoarthritic patient chondrocytes, comparable to the knockdown by the free ASO. The ability for gene silencing with the biomolecular assembly supports escape from an FcRn-driven endosomal recycling pathway and subsequent engagement with its mRNA target in the cytosol. In a similar manner, RNA interfering siRNA-GalNac conjugates achieves target gene silencing by likely escaping an asialoglycoprotein-mediated endosomal recycling pathway.[34] The mechanisms underlying escape from receptor-mediated endosomal pathways need to be investigated further.

Gapmer-mediated gene silencing commonly requires micromolar concentrations in the absence of a transfection reagent. In our work, significant gene silencing in osteoarthritis patient chondrocytes was achieved in the nanomolar range, which may be attributed to the specific sequence of the gapmer used. The level of silencing in this work is comparable to the silencing achieved at 500 nM in previous work performed with the same ASO sequence.[23] This result suggests that the functional integrity of ASO gene silencing is not compromised by inclusion into the biomolecular assembly that, in addition, also offers potential albumin-based half-life extension not exhibited by using ASO in its naked form.

Our "Plug-and-Play" design feature allows the ASO sequences to be switched for various disease applications using different sequences in the ODN module. The modular design can further be used to incorporate targeting ligands or additional drugs for combinatorial therapy. Furthermore, albumins engineered with additional thiols[35] could be used to maximize ASO payload. Next steps should involve investigations into the pharmacokinetics of assemblies in the double humanized FcRn/albumin (hFcRn$^{+/+}$, hAlb$^{+/+}$) mice representing a more physiological model for albumin-based drug designs[36] and therapeutic efficacy in an osteoarthritis model.

This work introduces a novel modular design that offers a versatile platform for potential improvements in delivery, biodistribution, and half-life of therapeutic ODNs.

■ ASSOCIATED CONTENT

Supporting Information

The Supporting Information is available free of charge at https://pubs.acs.org/doi/10.1021/acs.molpharmaceut.3c00561.

IEX-HPLC purification of the rHA-cODN conjugate and rHA-cODN/ASO assembly, fluorescence imaging of a native PAGE for dually labeled biomolecular assembly, MTT cytotoxicity assay of the biomolecular assembly, and detailed confocal microscopy images of the cellular internalization of the biomolecular assembly (PDF)

https://doi.org/10.1021/acs.molpharmaceut.3c00561
Mol. Pharmaceutics 2024, 21, 491−500

AUTHOR INFORMATION

Corresponding Author

Kenneth A. Howard − *Interdisciplinary Nanoscience Center (iNANO), Department of Molecular Biology and Genetics, Aarhus University, DK-8000 Aarhus C, Denmark;* orcid.org/0000-0002-9407-278X; Phone: +4587155831; Email: kenh@inano.au.dk

Authors

Marwa Elkhashab − *Interdisciplinary Nanoscience Center (iNANO), Department of Molecular Biology and Genetics, Aarhus University, DK-8000 Aarhus C, Denmark;* orcid.org/0000-0001-6386-7849

Yeter Dilek − *Department of Orthopedics, University Medical Center Utrecht, 3584 CT Utrecht, The Netherlands*

Morten Foss − *Interdisciplinary Nanoscience Center (iNANO), Aarhus University, DK-8000 Aarhus C, Denmark*

Laura B. Creemers − *Department of Orthopedics, University Medical Center Utrecht, 3584 CT Utrecht, The Netherlands;* orcid.org/0000-0002-1585-3052

Complete contact information is available at: https://pubs.acs.org/10.1021/acs.molpharmaceut.3c00561

Notes

The authors declare no competing financial interest.

ACKNOWLEDGMENTS

Funding: This project has received funding from the European Union's Horizon 2020 research and innovation programme under the Marie Skłodowska Curie grant agreement No 955335, the Turkish Government SDC8GW2SRBXDRZM, and the Dutch Arthritis Association (LLP12). Graphical abstract was created with BioRender.com. Figures were modified with Inkscape software.

REFERENCES

(1) Dhuri, K.; Bechtold, C.; Quijano, E.; Pham, H.; Gupta, A.; Vikram, A.; Bahal, R. Antisense Oligonucleotides: An Emerging Area in Drug Discovery and Development. *J. Clin. Med.* **2020**, *9* (6), No. 2004.

(2) Roberts, T. C.; Langer, R.; Wood, M. J. A. Advances in oligonucleotide drug delivery. *Nat. Rev. Drug Discovery* **2020**, *19* (10), 673−694.

(3) Gagliardi, M.; Ashizawa, A. T. The Challenges and Strategies of Antisense Oligonucleotide Drug Delivery. *Biomedicines* **2021**, *9* (4), No. 433.

(4) Migliorati, J. M.; Liu, S.; Liu, A.; Gogate, A.; Nair, S.; Bahal, R.; et al. Absorption, distribution, metabolism, and excretion of FDA-approved antisense oligonucleotide drugs. *Drug Metab. Dispos.* **2022**, *50* (6), 888−897.

(5) Yoo, B. H.; Bochkareva, E.; Bochkarev, A.; Mou, T. C.; Gray, D. M. 2′-O-methyl-modified phosphorothioate antisense oligonucleotides have reduced non-specific effects in vitro. *Nucleic Acids Res.* **2004**, *32* (6), 2008−2016.

(6) Geary, R. S.; Watanabe, T. A.; Truong, L.; Freier, S.; Lesnik, E. A.; Sioufi, N. B.; et al. Pharmacokinetic properties of 2′-O-(2-methoxyethyl)-modified oligonucleotide analogs in rats. *J. Pharmacol. Exp. Ther.* **2001**, *296* (3), 890−897.

(7) Soifer, H. S.; Koch, T.; Lai, J.; Hansen, B.; Hoeg, A.; Oerum, H.et al. Silencing of Gene Expression by Gymnotic Delivery of Antisense Oligonucleotides. In *Functional Genomics: Methods and Protocols*; Kaufmann, M.; Klinger, C., Eds.; Springer New York: New York, NY, 2012; pp 333−346.

(8) Stein, C. A.; Hansen, J. B.; Lai, J.; Wu, S.; Voskresenskiy, A.; Høg, A.; et al. Efficient gene silencing by delivery of locked nucleic acid antisense oligonucleotides, unassisted by transfection reagents. *Nucleic Acids Res.* **2010**, *38* (1), No. e3.

(9) Geary, R. S.; Norris, D.; Yu, R.; Bennett, C. F. Pharmacokinetics, biodistribution and cell uptake of antisense oligonucleotides. *Adv. Drug Delivery Rev.* **2015**, *87*, 46−51.

(10) Geary, R. S. Antisense oligonucleotide pharmacokinetics and metabolism. *Expert Opin. Drug Metab. Toxicol.* **2009**, *5* (4), 381−391.

(11) Yu, R. Z.; Kim, T.-W.; Hong, A.; Watanabe, T. A.; Gaus, H. J.; Geary, R. S. Cross-Species Pharmacokinetic Comparison from Mouse to Man of a Second-Generation Antisense Oligonucleotide, ISIS 301012, Targeting Human Apolipoprotein B-100. *Drug Metab. Dispos.* **2007**, *35* (3), 460−468.

(12) Hvam, M. L.; Cai, Y.; Dagnæs-Hansen, F.; Nielsen, J. S.; Wengel, J.; Kjems, J.; Howard, K. A. Fatty Acid-Modified Gapmer Antisense Oligonucleotide and Serum Albumin Constructs for Pharmacokinetic Modulation. *Mol. Ther.* **2017**, *25* (7), 1710−1717.

(13) Sleep, D.; Cameron, J.; Evans, L. R. Albumin as a versatile platform for drug half-life extension. *Biochim. Biophys. Acta, Gen. Subj.* **2013**, *1830* (12), 5526−5534.

(14) Schmidt, E. G. W.; Hvam, M. L.; Antunes, F.; Cameron, J.; Viuff, D.; Andersen, B.; et al. Direct demonstration of a neonatal Fc receptor (FcRn)-driven endosomal sorting pathway for cellular recycling of albumin. *J. Biol. Chem.* **2017**, *292* (32), 13312−13322.

(15) Pilati, D.; Howard, K. A. Albumin-based drug designs for pharmacokinetic modulation. *Expert Opin. Drug Metab. Toxicol.* **2020**, *16* (9), 783−795.

(16) Larsen, M. T.; Kuhlmann, M.; Hvam, M. L.; Howard, K. A. Albumin-based drug delivery: harnessing nature to cure disease. *Mol. Cell. Ther.* **2016**, *4* (1), No. 3.

(17) Nilsen, J.; Trabjerg, E.; Grevys, A.; Azevedo, C.; Brennan, S. O.; Stensland, M.; et al. An intact C-terminal end of albumin is required for its long half-life in humans. *Commun. Biol.* **2020**, *3* (1), No. 181.

(18) Andersen, J. T.; Dalhus, B.; Cameron, J.; Daba, M. B.; Plumridge, A.; Evans, L.; et al. Structure-based mutagenesis reveals the albumin-binding site of the neonatal Fc receptor. *Nat. Commun.* **2012**, *3* (1), No. 610.

(19) Larsen, M. T.; Rawsthorne, H.; Schelde, K. K.; Dagnæs-Hansen, F.; Cameron, J.; Howard, K. A. Cellular recycling-driven in vivo half-life extension using recombinant albumin fusions tuned for neonatal Fc receptor (FcRn) engagement. *J. Controlled Release* **2018**, *287*, 132−141.

(20) Caspersen, M. B.; Kuhlmann, M.; Nicholls, K.; Saxton, M. J.; Andersen, B.; Bunting, K.; et al. Albumin-based drug delivery using cysteine 34 chemical conjugates − important considerations and requirements. *Ther. Delivery* **2017**, *8* (7), 511−519.

(21) Kuhlmann, M.; Hamming, J. B. R.; Voldum, A.; Tsakiridou, G.; Larsen, M. T.; Schmøkel, J. S.; et al. An Albumin-Oligonucleotide Assembly for Potential Combinatorial Drug Delivery and Half-Life Extension Applications. *Mol. Ther. - Nucleic Acids* **2017**, *9*, 284−293.

(22) Dinesen, A.; Winther, A.; Wall, A.; Märcher, A.; Palmfeldt, J.; Chudasama, V.; et al. Albumin Biomolecular Drug Designs Stabilized through Improved Thiol Conjugation and a Modular Locked Nucleic Acid Functionalized Assembly. *Bioconjugate Chem.* **2022**, *33* (2), 333−342.

(23) Garcia, J. P.; Stein, J.; Cai, Y.; Riemers, F.; Wexselblatt, E.; Wengel, J.; et al. Fibrin-hyaluronic acid hydrogel-based delivery of antisense oligonucleotides for ADAMTS5 inhibition in co-delivered and resident joint cells in osteoarthritis. *J. Controlled Release* **2019**, *294*, 247−258.

(24) Rinaldi, C.; Wood, M. J. A. Antisense oligonucleotides: the next frontier for treatment of neurological disorders. *Nat. Rev. Neurol.* **2018**, *14* (1), 9−21.

(25) Matsui, S.; Aida, H. Hydrolysis of some N-alkylmaleimides. *J. Chem. Soc., Perkin Trans. 2* **1978**, No. 12, 1277−1280.

(26) Wetzel, R.; Becker, M.; Behlke, J.; Billwitz, H.; Böhm, S.; Ebert, B.; et al. Temperature behaviour of human serum albumin. *Eur. J. Biochem.* **1980**, *104* (2), 469−478.

(27) Rabe, K. S.; Niemeyer, C. M. Selective covalent conjugation of phosphorothioate DNA oligonucleotides with streptavidin. *Molecules* **2011**, *16* (8), 6916−6926.
(28) Nishina, T.; Numata, J.; Nishina, K.; Yoshida-Tanaka, K.; Nitta, K.; Piao, W.; et al. Chimeric Antisense Oligonucleotide Conjugated to α-Tocopherol. *Mol. Ther. - Nucleic Acids* **2015**, *4* (1), No. e220.
(29) Pendergraff, H. M.; Krishnamurthy, P. M.; Debacker, A. J.; Moazami, M. P.; Sharma, V. K.; Niitsoo, L.; et al. Locked Nucleic Acid Gapmers and Conjugates Potently Silence ADAM33, an Asthma-Associated Metalloprotease with Nuclear-Localized mRNA. *Mol. Ther. - Nucleic Acids* **2017**, *8*, 158−168.
(30) Asami, Y.; Nagata, T.; Yoshioka, K.; Kunieda, T.; Yoshida-Tanaka, K.; Bennett, C. F.; et al. Efficient Gene Suppression by DNA/DNA Double-Stranded Oligonucleotide In Vivo. *Mol. Ther.* **2021**, *29* (2), 838−847.
(31) Lauková, L.; Konečná, B.; Janovičová, L'.; Vlková, B.; Celec, P. Deoxyribonucleases and Their Applications in Biomedicine. *Biomolecules* **2020**, *10* (7), No. 1036.
(32) Petersen, S. S.; Kläning, E.; Ebbesen, M. F.; Andersen, B.; Cameron, J.; Sørensen, E. S.; Howard, K. A. Neonatal Fc Receptor Binding Tolerance toward the Covalent Conjugation of Payloads to Cysteine 34 of Human Albumin Variants. *Mol. Pharmaceutics* **2016**, *13* (2), 677−682.
(33) Schmøkel, J.; Voldum, A.; Tsakiridou, G.; Kuhlmann, M.; Cameron, J.; Sørensen, E. S.; et al. Site-selective conjugation of an anticoagulant aptamer to recombinant albumins and maintenance of neonatal Fc receptor binding. *Nanotechnology* **2017**, *28* (20), No. 204004.
(34) Brown, C. R.; Gupta, S.; Qin, J.; Racie, T.; He, G.; Lentini, S.; et al. Investigating the pharmacodynamic durability of GalNAc−siRNA conjugates. *Nucleic Acids Res.* **2020**, *48* (21), 11827−11844.
(35) Schelde, K. K.; Nicholls, K.; Dagnæs-Hansen, F.; Bunting, K.; Rawsthorne, H.; Andersen, B.; et al. A new class of recombinant human albumin with multiple surface thiols exhibits stable conjugation and enhanced FcRn binding and blood circulation. *J. Biol. Chem.* **2019**, *294* (10), 3735−3743.
(36) Viuff, D.; Antunes, F.; Evans, L.; Cameron, J.; Dyrnesli, H.; Ravn, B. T.; et al. Generation of a double transgenic humanized neonatal Fc receptor (FcRn)/albumin mouse to study the pharmacokinetics of albumin-linked drugs. *J. Controlled Release* **2016**, *223*, 22−30.

https://doi.org/10.1021/acs.molpharmaceut.3c00561
Mol. Pharmaceutics 2024, 21, 491−500